ISSUES OF UNCERTAINTY REGARDING LOCALIZED STRAINS IN GRANULAR SOILS

M.A. Mooney[1] A.M. ASCE, R.J. Finno[2] M. ASCE,
G. Viggiani[2], W.W. Harris[3] A.M. ASCE

Abstract

Shear bands or slip zones occur frequently in field situations and in laboratory experiments involving soils. Once a shear band has formed, the stability of the overlying structure is governed by the strength and deformation properties of the material within the localized zone. This paper discusses the use and mis-use of continuum-based deformation analysis techniques to characterize shear band deformation. Results are presented illustrating that previously used continuum-based techniques are significantly affected by the erratic nature of particulate behavior. A deformation analysis technique utilizing a least squares linear regression approach is incorporated to minimize the effects of particulate behavior when determining shear band strains. Results are also presented indicating that the use of a small strain formulation can result in erroneously excessive dilation within a shear band.

Introduction

The concentration of strain into narrow zones, i.e. shear bands or slip zones, commonly occurs in field situations and in laboratory experiments involving soils. Once a shear band has formed, the stability and deformation of the overlying material is governed by the strength and deformation properties of the material within the localized zone. To date, experimental investigations of shear band behavior have been complemented

[1]School of Civil Engrg. and Env. Science, Univ. of Oklahoma, Norman, OK 73019
[2]Department of Civil Engrg., Northwestern Univ., Evanston, IL, 60208
[3]Department of Civil and Env. Engrg., Univ. of Alabama, Tuscaloosa, AL 35487

by the use of local deformation analysis techniques. The accurate characterization of local strain behavior can lend significant insight into the mechanism of shear band deformation, the nature of undrained conditions in the presence of shear banding, and the achievement of critical state within the zone of localized strain. Stereophotogrammetry is one technique which has been used to characterize local deformation behavior during plane strain experiments of granular material (Butterfield et al. 1970, Desrues et al. 1985, Mokni 1992, Yoshida et al. 1994, Harris et al. 1995). In addition to providing qualitative shear band characteristics, stereo-based analyses have been carried out to quantify local strain behavior using displacements of either sand grains or grid points painted on a membrane. These stereo-based techniques adopt a continuum-like approach by assuming a linear interpolation between three nodal or sand grain displacements. However, strains based on the displacements of a few grains are greatly affected by the erratic nature of particulate behavior and can be incorrect (Mooney 1996).

This paper discusses the use and mis-use of continuum-based methods when characterizing local deformation behavior of a particulate medium. A deformation analysis technique utilizing a least squares linear regression approach was developed to minimize the effects of particulate behavior when determining strains (Mooney 1996). This probability-based regression method is capable of determining both the local deformation behavior and the accuracy with which the method can report strains. Herein, the ability of the regression approach to capture 'true' deformation behavior is evaluated during the homogeneous portion of a plane strain compression test, i.e. prior to strain localization. The limitations of an infinitesimal strain formulation when characterizing shear band deformation is also discussed. In previous work (Harris et al 1995, Yoshida et al. 1994), local deformation analysis has been performed based on the assumption of infinitesimal strain. It will be shown herein that the use of a small strain formulation to evaluate shear band behavior can result in erroneously excessive dilation.

Experimental Program

Plane strain compression tests were performed on specimens of loose, saturated masonry sand under displacement-control. Specimens consisted of masonry sand, a clean, subrounded to subangular quartz sand, with mean grain diameter, D_{50}, of 0.32

mm and a coefficient of uniformity, $C_u=D_{60}/D_{10}$, of 1.3. The presence of different colored grains assisted in the identification of individual points for deformation analysis.

Photographs of the deforming specimen were taken from a fixed camera position through a clear Plexiglas sidewall to record the development and progression of strain localization. The features of this system as well as the photographic technique are detailed by Harris et al. (1995) and are briefly summarized herein. Figure 1 shows the plane of deformation, which is the camera view, of a 140 mm tall by 40 mm wide specimen. The transverse dimension (section A-A) of the specimen, fixed by lubricated sidewalls to achieve plane strain while minimizing friction, is 80 mm. The sample rests vertically between two oversized, lubricated platens. The axial load is measured both by an upper load cell (F_1 in Fig. 1) and three lower load cells (F_2,F_3,F_4), while the out-of-plane load is measured by four load cells embedded in one sidewall (F_5 through F_8). Pore water pressure is measured at the top (p_1) and bottom (p_2) of the specimen by pressure transducers. LVDT's are incorporated to measure axial displacement and possible tilt of the specimen (u_1, u_2), as well as lateral movements of the specimen (u_3 through u_6) and sled displacement (u_7) in the plane of deformation. The bottom platen rests on a linear sled, which can either be locked to prohibit movement or unlocked to allow kinematically unrestrained shear band deformation in the x-direction. It should be noted that shear bands formed irrespective of the sled condition (Finno et al. 1996a).

Figure 1 Plane Strain Apparatus

Evaluation of Shear Band Deformation

When two photographs of a deforming specimen are viewed in stereo, displaced regions appear elevated, with the elevation proportional to the magnitude of relative displacement. In the presence of a shear band, the deforming specimen appears as two planes of different elevation connected by a slope, as illustrated in Figure 2a. The sloped area is the expression of the shear band, with a corresponding width of 10 to 20 times the mean grain diameter. The stereo view provides a guide for the selection of sand grains for deformation analysis. The coordinates of selected grains are determined on each photograph by digitization using a standard desktop tablet. Assuming a continuum-based approach, Green-Lagrange finite strain components, $\boldsymbol{\varepsilon}$, can be determined as:

$$\varepsilon_x = \frac{\partial \boldsymbol{u}_1}{\partial x_1} + \frac{1}{2}\left[\left(\frac{\partial \boldsymbol{u}_1}{\partial x_1}\right)^2 + \left(\frac{\partial \boldsymbol{u}_2}{\partial x_1}\right)^2\right]$$

$$\varepsilon_y = \frac{\partial \boldsymbol{u}_2}{\partial x_2} + \frac{1}{2}\left[\left(\frac{\partial \boldsymbol{u}_1}{\partial x_2}\right)^2 + \left(\frac{\partial \boldsymbol{u}_2}{\partial x_2}\right)^2\right] \qquad (1)$$

$$\varepsilon_{xy} = \frac{1}{2}\left[\frac{\partial \boldsymbol{u}_1}{\partial x_2} + \frac{\partial \boldsymbol{u}_2}{\partial x_1} + \left(\frac{\partial \boldsymbol{u}_1}{\partial x_1}\frac{\partial \boldsymbol{u}_1}{\partial x_2}\right) + \left(\frac{\partial \boldsymbol{u}_2}{\partial x_1}\frac{\partial \boldsymbol{u}_2}{\partial x_2}\right)\right]$$

where $\boldsymbol{u}_1$ and $\boldsymbol{u}_2$ are the displacement functions in the x_1 and x_2 directions, respectively. The x_1 and x_2 directions can be any orthogonal coordinate system in the plane of deformation. Note that since the specimen is undergoing plane strain deformation, the out-of-plane displacement $\boldsymbol{u}_3$ is zero. Invariant measures of volumetric and shear strain are given as:

$$\varepsilon_{vol} = -\left[\frac{\partial \boldsymbol{u}_1}{\partial x_1} + \frac{\partial \boldsymbol{u}_2}{\partial x_2} + \left(\frac{\partial \boldsymbol{u}_1}{\partial x_1}\frac{\partial \boldsymbol{u}_2}{\partial x_2}\right) - \left(\frac{\partial \boldsymbol{u}_1}{\partial x_2}\frac{\partial \boldsymbol{u}_2}{\partial x_1}\right)\right] \qquad (2)$$

$$\varepsilon_{sh} = \frac{\sqrt{2}}{3}\left[\varepsilon_x^2 + \varepsilon_y^2 + (\varepsilon_x - \varepsilon_y)^2 + 6\varepsilon_{xy}^2\right]^{1/2} \qquad (3)$$

In previous work, Harris et al. (1995) computed strains based on the linear interpolation of three nodal displacements. The grains used to define three-noded elements were chosen such that each element would span the width of the shear band (see Fig. 2b). In an attempt to characterize the deformation response while limiting erratic particulate behavior, a least squares linear regression method was developed (Mooney 1996). The basis for this probability-based approach stems from the stereophotogrammetric view, wherein a shear band of finite

width appears smooth and linear (see Fig. 2a). This suggests that a unique, linear displacement function is sufficient to characterize local shear band deformation. The aim of the method is to reduce the effect of the erratic nature of particulate behavior on the determined values of strain by incorporating a sufficient number of displacement measurements in a region for regression analysis. For example, it was found that 15 to 18 sand grains were sufficient to uniquely define the strain behavior over an area of 40 mm^2 within the shear band.

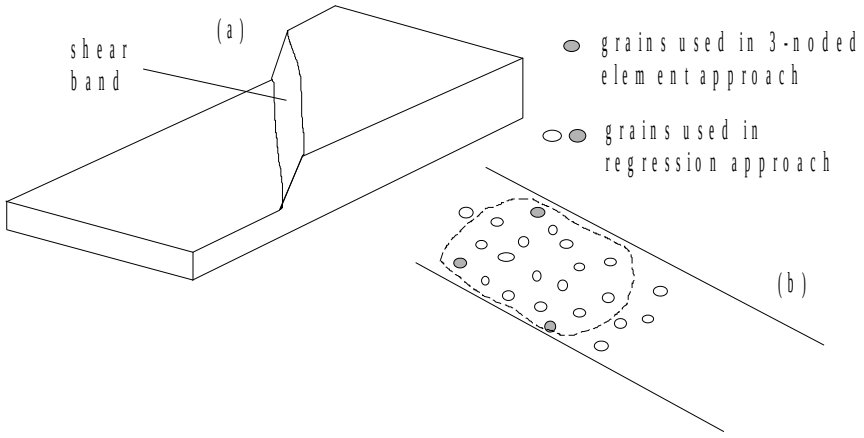

Figure 2 (a) Shear band as viewed through stereoscope, (b) Selection of grains for deformation analysis

Local deformation analysis requires grain displacements to be decomposed into two orthogonal components $\boldsymbol{u}_1$ and $\boldsymbol{u}_2$. To determine the displacement function over a region, a least squares linear regression analysis is performed on each discrete set of displacement components, $\boldsymbol{u}_1$ and $\boldsymbol{u}_2$:

$$\boldsymbol{u}_j = \boldsymbol{X}\boldsymbol{\Omega}_j + \boldsymbol{r}_j \tag{4}$$

$$\boldsymbol{u}_j = \begin{bmatrix} u_{1j} \\ u_{2j} \\ \vdots \\ u_{nj} \end{bmatrix}, \quad \boldsymbol{X} = \begin{bmatrix} 1 & x_{11} & x_{12} \\ 1 & x_{21} & x_{22} \\ \vdots & \vdots & \vdots \\ 1 & x_{n1} & x_{n2} \end{bmatrix}, \quad \boldsymbol{\Omega}_j = \begin{bmatrix} \Omega_{0j} \\ \Omega_{1j} \\ \Omega_{2j} \end{bmatrix}, \text{ and } \boldsymbol{r}_j = \begin{bmatrix} r_{1j} \\ r_{2j} \\ \vdots \\ r_{nj} \end{bmatrix}$$

where u_{ij} and x_{ij} are the displacement and regressor variables, respectively, of the i-th particle in the j-th direction and n is the number of discretized grains. The regressor variables x_{ij} are the initial coordinates of the sand grains and the least squares estimators are given by $\boldsymbol{\Omega}_j$. The residual, $\boldsymbol{r}_j$, contains the differences between the observed and predicted displacements of each grain. The principle of the least squares method is to

determine a 'best fit' of the data while minimizing the sum of the squares of the residual. The fitted displacement function is given by:

$$\boldsymbol{u}_j = \boldsymbol{X}\Omega_j = \boldsymbol{X}\left(\boldsymbol{X}^T\boldsymbol{X}\right)^{-1}\boldsymbol{X}^T\boldsymbol{u}_j \tag{5}$$

A regression analysis is performed on a sample with the purpose of predicting the behavior of the population. The least square estimators $\boldsymbol{\Omega}_j$ are unbiased estimators of the corresponding population values and relate directly to the derivatives of the fitted displacement function, i.e. for a given fit:

$$\begin{aligned}\boldsymbol{u}_1 &= \Omega_{01} + \Omega_{11}x_1 + \Omega_{21}x_2\\ \boldsymbol{u}_2 &= \Omega_{02} + \Omega_{12}x_1 + \Omega_{22}x_2\end{aligned} \tag{6}$$

Due to the uncertainty involved in attempting to apply a continuum-based approach to a particulate medium, one advantage of the regression analysis is that it provides a statistical summary of the analysis. The sample variances associated with the least squares estimators $\boldsymbol{\Omega}_j$ are given by the diagonals of the covariance matrix:

$$Cov\left(\Omega_j\right) = \sigma^2\left(\boldsymbol{X}^T\boldsymbol{X}\right)^{-1} \tag{7}$$

where σ^2 is the variance of the displacement fit (see Mooney 1996). The off-diagonals or sample covariance terms were much less than the variance terms and therefore were not considered. With the determined variances of the least squares estimators, the accuracy of calculated strains can be reported. Given that *Y* is a function of several random variables, $g(X_1, X_2, \ldots X_n)$, the variance of *Y* can be obtained as a first order approximation by:

$$Var(Y) = \sum_{i=1}^{n}\left(\frac{\partial g}{\partial X_i}\right)^2 Var(X_i) \tag{8}$$

where the partial derivatives are evaluated at their mean, $\overline{X}_i$. For example,

$$Var\left[\varepsilon_x\right] = \left(1 + \left(\frac{\partial \boldsymbol{u}_1}{\partial x_1}\right)^2\right)Var\left[\frac{\partial \boldsymbol{u}_1}{\partial x_1}\right] + \left(\frac{\partial \boldsymbol{u}_2}{\partial x_2}\right)^2 Var\left[\frac{\partial \boldsymbol{u}_2}{\partial x_2}\right] \tag{9}$$

The variance associated with other components of strain follow from equation (8). For a detailed description of the regression method as well as the determination of accuracy and goodness of fit, see Mooney (1996).

Experimental Results

Detailed analysis of the testing program is given by Finno et al. (1996a, 1996b). To provide the reader with the basic

responses from these unconventional experiments, Figures 3, 4, and 5 illustrate the results obtained from a typical plane strain experiment on a specimen of loose sand. This specimen, prepared by moist tamping to obtain a very loose state, was k_o consolidated (k_o=0.49) to a vertical effective stress of 225 kPa. The consolidated void ratio of test ms2 was 0.83 which corresponds to a relative density of 12%. The specimen was subsequently sheared under undrained conditions with an applied displacement rate of 1.7 mm/hr. Figure 3 shows the lateral deformation response recorded by LVDTs placed as shown in Figure 1. Note that during test ms2, the sled was locked in place. Since the specimen is subjected to undrained plane strain compression, the axial strain should equal the lateral strain as indicated by the dashed line in Figure 3a. Both the local lateral strain response, defined as the change in width between each pair of LVDTs divided by the consolidated width of the specimen, and the width difference between the upper and lower portions of the specimen indicate non-homogeneous deformation beginning at approximately 3.7% global axial strain, marked point O in Figure 3. At approximately 4.4% global axial strain, the response in Figure 3a indicates that a shear band has completely intersected the upper pair of LVDTs because the upper local lateral strain increases linearly while the lower local lateral strain remains essentially constant. The complete formation of the shear band is marked point B. When a shear band has intersected the upper pair of LVDTs, the upper local lateral strain response reduces to a measure of the relative horizontal displacement between the two portions of the specimen. The lower lateral strain response, however, remains as an appropriate measure of local lateral strain.

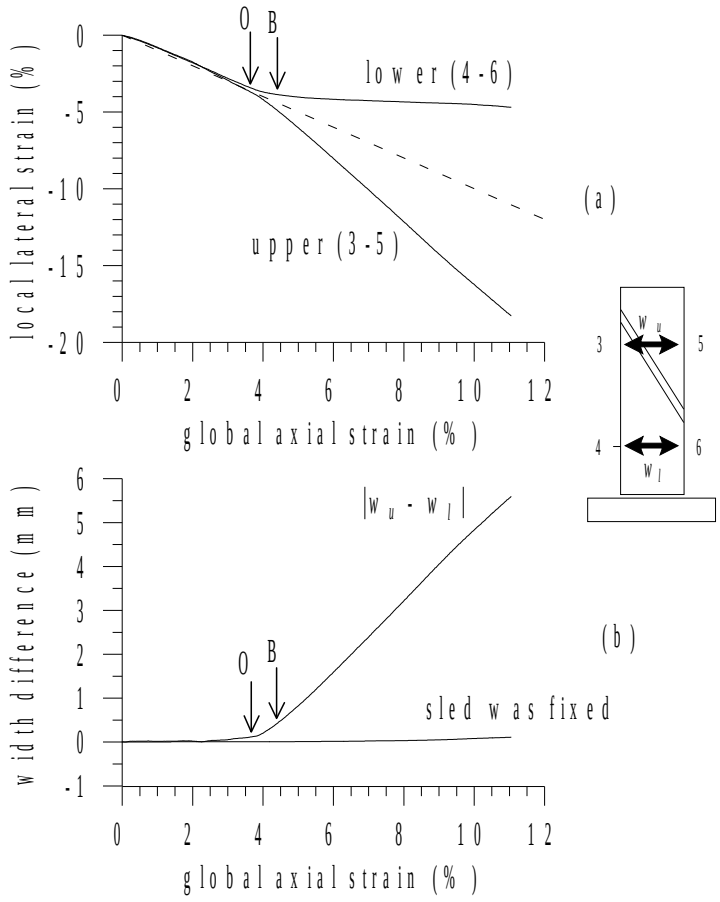

Figure 3 Lateral deformation response during shearing of test ms2: (a) local lateral strain, (b) width difference between upper and lower portions of specimen

The progression of strain localization as observed in stereo is shown in Figure 4. Within each block is the image obtained by stereoscopically viewing two photographs at the levels of global axial strain indicated below each block and on the axial load curve. The lines shown within each block represent the projection of the boundaries of the shear band as viewed in stereo. The stereophotogrammetric view indicates the formation of a persistent shear band during the increment 4-5. Although not evident in test ms2, temporary modes of strain localization often preceded the formation of a persistent shear band (Finno et al. 1996a). The shear band in Figure 4 is initially inclined at an angle of 48° from the direction of the minor principal stress (horizontal) but thereafter becomes steeper (57°). The thickness of the shear band is approximately 5 to 6 mm, corresponding to 16 to 20 times the mean grain diameter. The lines within the shear band during increments 8-9, 9-10, and 10-11 indicate a

change in slope within the localized zone. The shear band, which is uniform throughout its early progression becomes non-uniform during the latter increments.

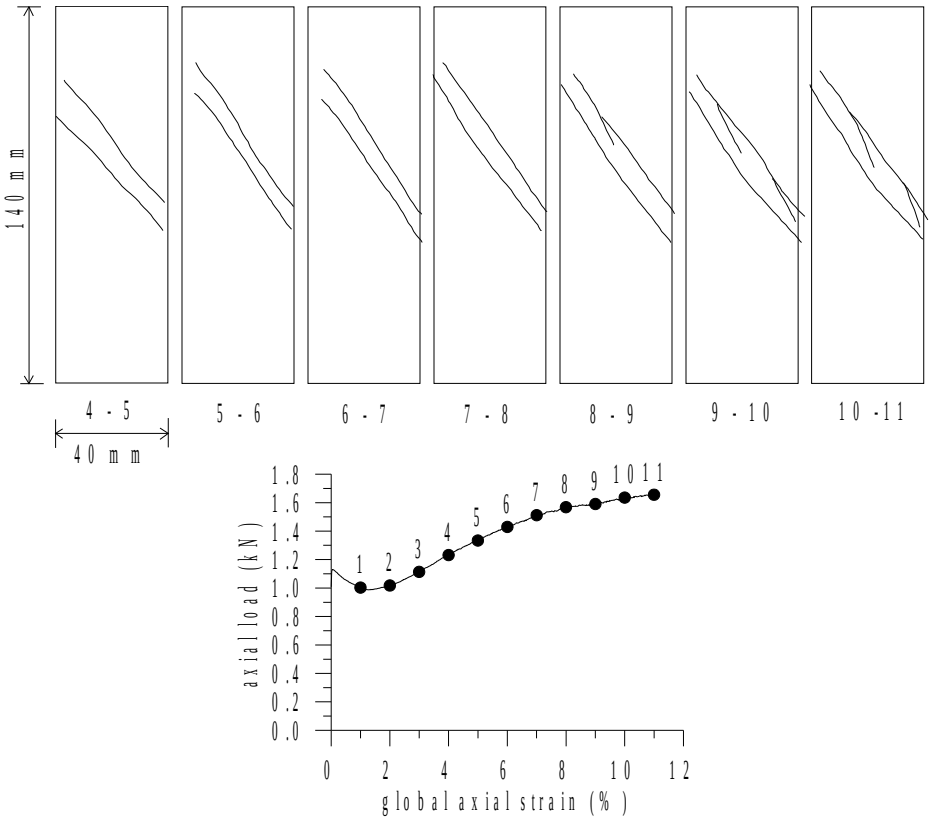

Figure 4 Evolution of strain localization observed during test ms2

The stress-strain response for test ms2 is shown in Figure 5. Measures of shear stress, q, and mean effective stress, p', are given as:

$$q = \frac{1}{\sqrt{2}}\left[(\sigma_1 - \sigma_2)^2 + (\sigma_1 - \sigma_3)^2 + (\sigma_2 - \sigma_3)^2\right]^{\frac{1}{2}}$$

$$p' = \frac{1}{3}(\sigma_1' + \sigma_2' + \sigma_3') \quad (10)$$

where σ_1, σ_2, and σ_3 correspond to the vertical, out-of-plane horizontal, and in-plane horizontal stresses, respectively. The prime refers to effective stress. The reduction in shearing

resistance at very small strains along with the monotonic increase in excess pore water pressure (Fig. 5a) is typical of contractive sand sheared undrained from a k_o condition. Points O and B on Figure 5 indicate the onset of strain localization and full formation of a persistent shear band as determined from local lateral strain response. Test ms2 undergoes significant shear strength reduction but rehardens prior to both a reduction in excess pore

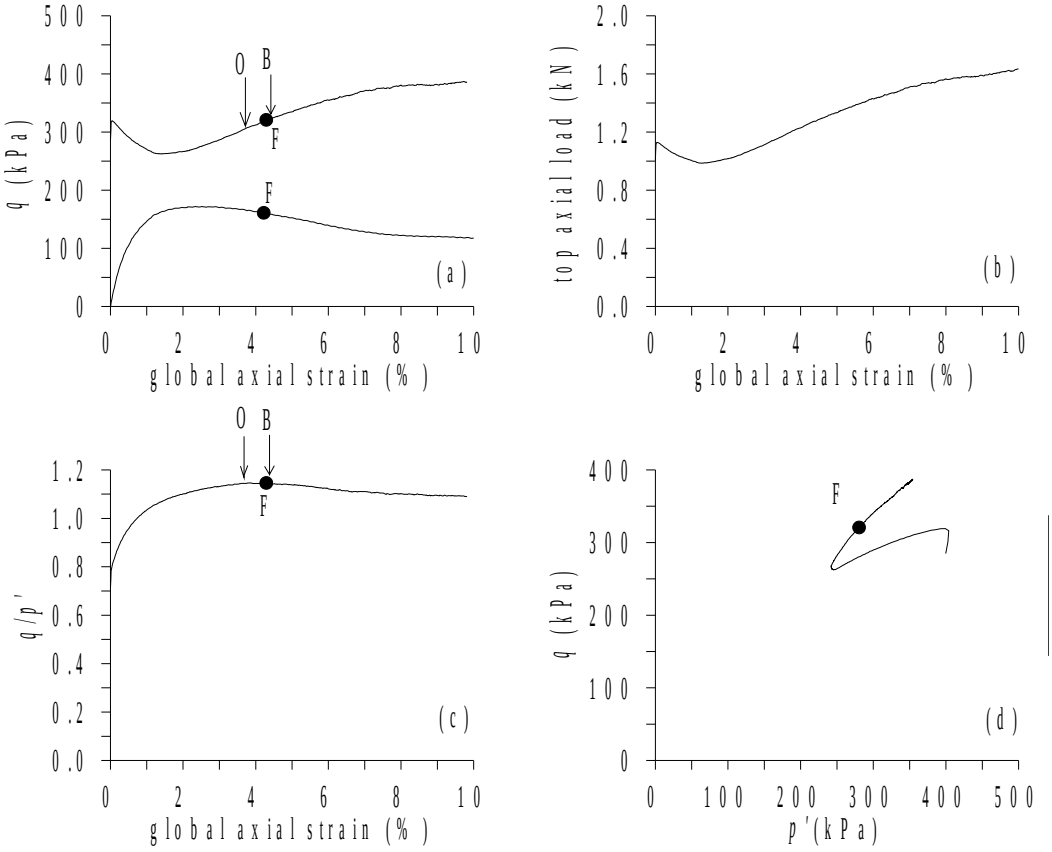

Figure 5 Stress-strain response during shearing of test ms2: (a) deviator stress and excess pwp, (b) top and bottom axial load,
(c) effective stress ratio, and (d) effective stress path

water pressure and the occurrence of strain localization, as indicated in Figure 5a. The onset of strain localization (point O), followed by the peak mobilized friction (point F), and subsequent complete formation of a shear band (point B) was a pattern observed in all tests (Finno et al. 1996a). The specimen is exhibiting globally dilative behavior during the onset of strain localization as indicated by the reduction in excess pore water pressure.

It is generally assumed that prior to the onset of strain localization, the specimen is behaving in an elemental fashion, i.e. the specimen is undergoing homogeneous deformation. The ability of stereo-based methods to characterize local deformation can be evaluated during the homogeneous portion of a test when the global response is representative of elemental behavior. An investigation of the ability of both the 3-node element method and the regression method to characterize the strains was performed. Since the true objective of the stereo-based methods is to characterize strains within a shear band, an area of comparable size was selected for analysis (see Fig. 6). For the 3-node element analysis, strain values of 10 elements were determined within the chosen area. Each element consisted of different sand grains as shown on the inset. Plotted in Figure 6 are the axial, lateral, and volumetric strains as determined from the analysis. The solid line represents the globally-determined values of strain. As illustrated, there is significant scatter in the results obtained from the 3-noded elements due to the effect of erratic particulate behavior. In fact the erratic behavior dominates the resulting strain values.

Also shown in Figure 6 are the components of strain as determined by the linear regression method. Regression analysis was performed over 18 sand grain displacements in the area shown. The error bars indicate the standard error associated with the determined values of strain. As shown in Figures 6a and 6b, the regression approach predicts the axial and lateral strains quite well up until 4% global axial strain. As the deformation becomes concentrated within the shear band, the components of strain in the area analyzed reach a limit value and are no longer comparable to global response. Figure 6c illustrates the limitation of the regression analysis in predicting volumetric strain, which is globally equal to zero during this undrained test. As illustrated by the standard errors, detecting volume changes smaller than approximately 1 to 1.5% are beyond the capability of the regression approach. Note that the scatter in volumetric strain from the 3-noded element approach is ±3 to 4%.

Figure 7 shows the volumetric and shear strains which develop within the fully formed shear band of test ms2 as determined by the regression method. The regression analysis was performed over two individual regions, each consisting of 15 grain displacements, and over the combined regions. The global axial strain values noted in Figure 7 provide a relationship to the axial load. Figure 7 illustrates the magnitude of shear strains

achieved (≈ 55%), thus confirming the need for a finite strain formulation. The standard errors

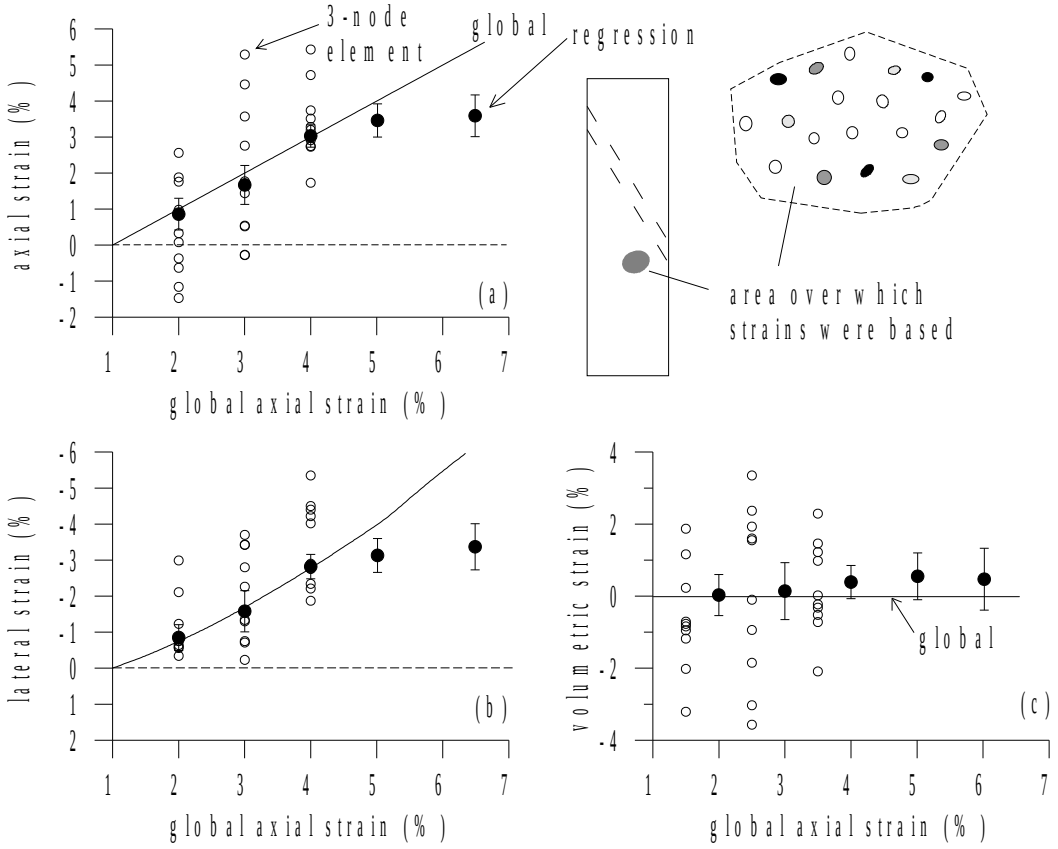

Figure 6 Comparison of strains computed globally, by regression analysis, and by 3-noded elements: (a) axial strain, (b) lateral strain, (c) volumetric strain

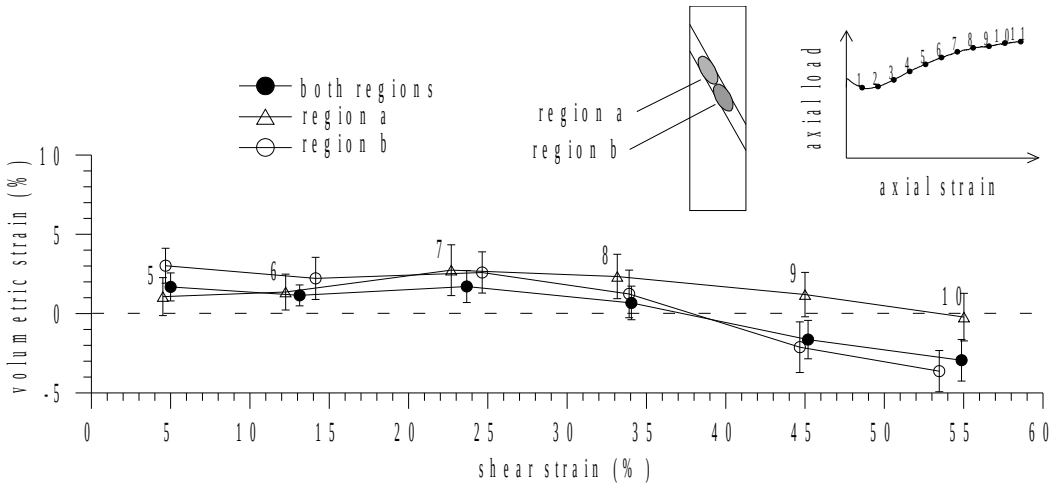

Figure 7 Volumetric and shear strains within shear band of test ms2

associated with the shear strains shown are less than 1%. The volumetric strains achieved in the shear band are very small in comparison with the shear strains. The localized zone shows a slight initial compression, a period of constant volume, and a tendency to dilate from 8% global axial strain onward. Given the standard errors associated with the volumetric and shear strains, Figure 7 shows that there is very little difference in shear deformation behavior between the two regions and a slight difference in volumetric strain behavior. This response coupled with a reduction in excess pore water pressure and an increasing axial load (Fig. 5) suggests the possibility of local drainage and fluid flow during a globally undrained test.

Due to the intense level of shear strain within a localized zone, the use of an infinitesimal strain approximation can lead to incorrect results. This is illustrated in Figure 8 by the difference in observed shear band deformation response during tests ms2 and ms3 determined by both finite strain and infinitesimal strain formulations using 3-node element analysis. The results were determined from the same chosen elements, therefore the relative effect of erratic particle response is eliminated. As illustrated, the small strain approximation indicates cumulative dilation within the shear band on the order of 15% during test ms3

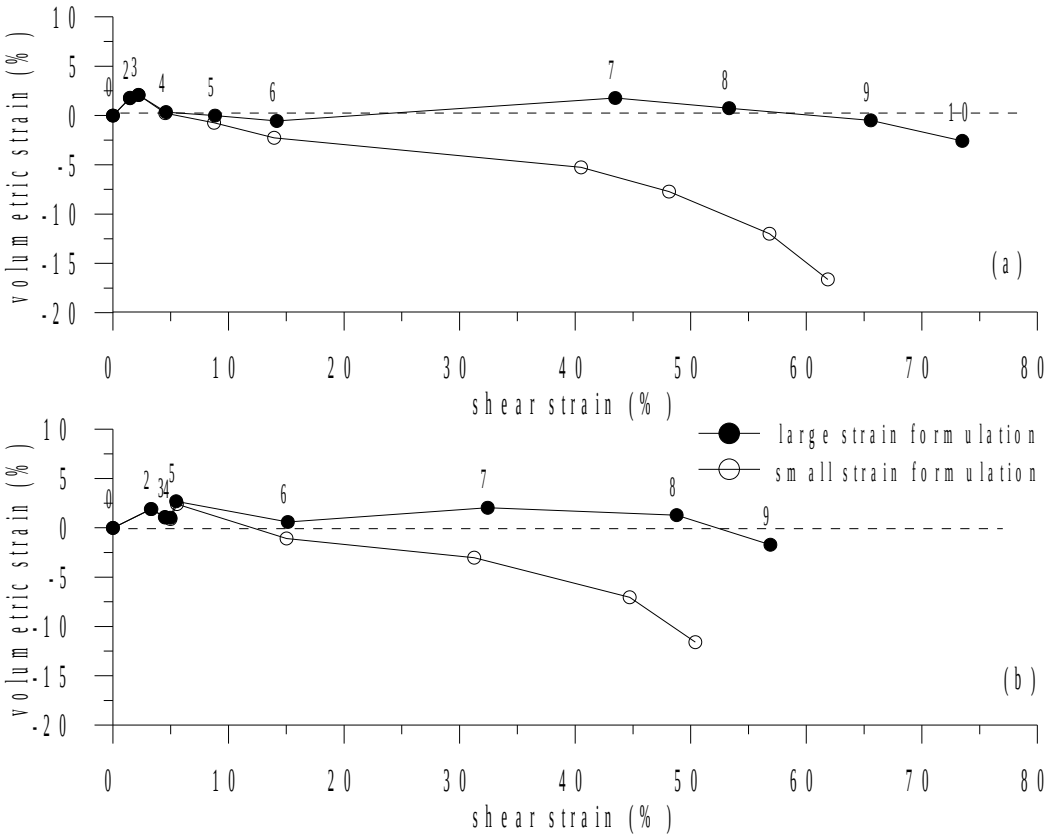

Figure 8 Volumetric and shear strains based on large strain and small strain

and 12% during test ms2, whereas the finite strain approach indicates that there is essentially no change in volume within the shear band throughout the test. Bardet and Proubet (1991) also noted the over-prediction of dilation when using a small strain formulation during numerical simulations of strain localization. Resolution of this discrepancy is critical because such magnitudes of dilation in the shear band imply significant local volumetric expansion in a globally undrained test. Dilation on the order of 15% in a specimen with a consolidated void ratio of approximately 0.85 corresponds to an increase in void ratio of 0.3. This suggests the void ratio in the band at large strains is 1.15, which is a state that is highly improbable for a sand with a maximum void ratio of 0.875. Figure 8 also shows that the small strain formulation yields shear strains 15% and 20% less than the actual value in tests ms2 and ms3, respectively.

Concluding Remarks

Classical continuum-based mechanics was established on the fundamental notion that a material body possesses a continuous mass density. The application of a continuum-based deformation analysis technique depends on the representative area upon which the method is applied. Though sand is a particulate material and the thickness of a shear band is approximately one order of magnitude greater than mean grain diameter, the observation that the shear band in granular media is essentially smooth and planar when viewed in stereo indicates that a shear band is large enough such that a representative area can be found within a band. Therefore, if properly applied, a continuum-based approach can be used to document deformation behavior within a shear band.

The premise on which the regression approach was formed stems from the need to minimize the erratic nature of particulate behavior. Figure 6 illustrated the dominating effect that the particulate behavior can have on reported strains. Continuum-based deformation analysis techniques, which are based on the interpolation of a few displacements, highlight this erratic behavior and yield erroneous values of strain. The analysis shown in Figure 6 also illustrates the ability of the regression-based approach to not only minimize the particulate response, but to accurately depict the ‘true’ deformation behavior. The representative area used in the analysis of Figure 6 was comparable to a typical area within a shear band.

Notwithstanding erratic behavior, the approximation of small strain theory is invalid in a zone of such intense shearing. The application of an infinitesimal strain approximation to characterize shear band deformation can yield significant values of dilation which are incorrect. The infinitesimal strain approximation can also under predict the levels of shear strain accumulated in the zone of localized strain.

Acknowledgement

This work was partially supported by funds from grant BCS-9019755 from the National Science foundation. Their support for this research is gratefully acknowledged.

References

Bardet, J.P. and Proubet, J. (1991) - "A numerical investigation of the structure of persistent shear bands in granular media", *GŽotechnique*, Vol. 41, No. 4, pp. 599-613.

Butterfield, R., Harkness R.M. and Andrawes K.Z. (1970) - "A stereo-photogrammetric method for measuring displacements fields", *GŽotechnique*, Vol. 20, No. 3, pp. 308-314.

Desrues, J., Lanier, J. and Stutz, P. (1985) - "Localization of the deformation in tests on sand sample", *Engineering Fracture Mechanics*, Vol. 21, No. 4, pp. 909-921.

Finno, R.J., Harris, W.W., Mooney, M.A. and Viggiani, G. (1996a) "Shear bands in plane strain compression of loose sand", in press, *GŽotechnique*.

Finno, R.J., Harris, W.W., Mooney, M.A. and Viggiani, G. (1996b) "Strain localization and undrained steady state of sands", in press, *J. Geotechnical Engineering*, ASCE.

Harris, W.W., Viggiani, G., Mooney, M.A. and Finno, R.J. (1995) - "Use of stereophoto-grammetry to analyze the development of shear bands in sand", *Geotechnical Testing Journal*, ASTM, Vol. 18, No. 4, pp. 405-420.

Mokni, M. (1992) - "Relations entre dŽformations en masse et dŽformations localisŽes dans les matŽriaux granulaires", Thèse de Doctorat de l'UniversitŽ J. Fourier de Grenoble, France.

Mooney, M. A. (1996) "An experimental study of strain localization and the mechanical behavior of sand", Ph.D. Dissertation, Northwestern University, Evanston, IL.

Yoshida,T., Tatsuoka, F., Kamegai, Y., Siddiquee, M.S.A. and Park, C.-S. (1994) - "Shear banding in sands observed in plane strain compression", Proceedings of the 3rd International Workshop on Localisation and Bifurcation Theory for Soils and Rocks, Aussois, France, Balkema, Rotterdam, pp. 165-179.